Probe Calibration in Transient Microdialysis *In Vivo*

Peter M. Bungay,[1,3] Robert L. Dedrick,[1] Elizabeth Fox,[2] and Frank M. Balis[2]

Received November 2, 2000; accepted November 15, 2000

Purpose. We examine the theoretical basis for calibrating microdialysis probes *in vivo* for pharmacokinetic experiments in which the extracellular analyte concentrations vary in time.

Methods. A software package, MICRODIAL, was used to simulate microdialysis for illustrative transient situations with linear concentration dependence.

Results. For a constant distant extracellular analyte concentration, the calibration factor (extraction fraction, E_d) exhibits a mass transfer transient associated with the development of spatial concentration profiles within the tissue and the probe. Processes clearing the analyte from the extracellular fluid (ECF) strongly influence the rapidity of approach to steady-state and affect the magnitude of the steady-state calibration factor, E_d^{ss}. For situations in which the distant ECF concentration varies in time as a result of exchange with the plasma compartment, different time profiles of the distant ECF and plasma concentrations yield different transient E_d. For the linear, transient cases examined, the area-under-the-curve ($AUC_{0-\infty}$) time integral of the distant ECF concentration was found to be proportional to the outflow dialysate concentration-time integral with E_d^{ss} being the proportionality constant.

Conclusions. The options for calibrating microdialysis probes in solid tissues appear limited under non-steady state conditions; however, *AUC* integrals for linear systems may be determined by continuous microdialysis sampling and steady-state probe calibration approaches.

KEY WORDS: microdialysis; calibration; pharmacokinetics; area-under-the-curve; diffusion.

INTRODUCTION

Microdialysis has become a common technique for monitoring relative changes in the free concentration of drugs and other analytes in various tissues during *in vivo* studies. However, there are inherent limitations in using microdialysis to determine the time course of absolute analyte concentrations in transient experiments. The limitations relate to the time lag introduced by the necessary diffusional exchange of analyte between the probe perfusate, probe membrane and the surrounding tissue. The first practical limitation is that microdialysis can only follow extracellular fluid (ECF) concentration changes whose time scale is slower than this microdialysis diffusional transient. If the pharmacokinetic transient is much slower, then in principle, probes can be perfused at sufficiently low flow rates to maintain near equilibration of the analyte between the effluent dialysate and the tissue extracellular fluid. This requires adequate analytical sensitivity and appropriate sample handling techniques to assay the analyte in small sample volumes. In practice, perfusate-tissue equilibration is often either impracticable to achieve or undesirable. For nonequilibrium operation, a procedure for probe calibration *in vivo* is required to relate dialysate measurements to the concentration in the ECF. The constraints on determining the dialysate-ECF relationship constitute a second limitation to the use of microdialysis to study pharmacokinetic transients. Evaluating whether calibration is achievable depends upon a variety of factors, including the kind of information that is sought. In many studies of pharmacological or toxicological agents, the integral over time of compartment concentrations suffices in lieu of full temporal concentration profiles of the agent. The specific aims of this report are: (1) to examine some of the theoretical constraints to developing general calibration procedures for transient experiments, and (2) to suggest that the probe calibration requirements may be simplified when time-integral, or area-under-the-curve (*AUC*), information is the microdialysis objective.

METHODS

In the analysis of time-varying microdialysis experiments two kinds of transients need to be distinguished. The first is the mass transfer transient associated with the development of spatial concentration profiles in the probe and adjacent tissue. This transient is inherent to microdialysis, and is critically dependent upon the rates of processes clearing the analyte from the extracellular fluid (1–3). The second kind of transient might be termed a pharmacokinetic transient. This is a disturbance in the microdialysis behavior associated with temporal changes in the distant ECF analyte concentration, C_e^{∞}. Distant ECF changes are those which would occur in the absence of the probe and which result from analyte exchange with communicating compartments, such as the plasma or intracellular spaces. These two kinds of transients are coupled and should be considered simultaneously when both occur.

Mathematical models incorporating analyte clearance kinetics, and the mass transfer and pharmacokinetic transients, were proposed by Morrison *et al.* (1) and Morrison *et al.* (2) for systems that are linear in concentration and satisfy a number of other common assumptions. The transient model of Morrison *et al.* (2) and the steady-state model of Bungay *et al.* (4) have been programmed into the Macintosh application, MICRODIAL (5), to provide a tool to aid microdialysis users in planning and analyzing their experiments.

Pharmacokinetic transients are introduced in MICRODIAL through a lumped plasma compartment with a free analyte concentration, C_p, that is constrained to monoexponential variation in time, t. The exponential variation is prescribed by assigning values for the initial plasma concentration, C_{p0}, and the plasma decay constant, λ,

$$C_p = C_{p0} \cdot e^{-\lambda t}. \quad (1)$$

Linear exchange of the analyte occurs between the plasma and the ECF of the tissue containing the probe at a rate per gram of tissue given by, $k_{\text{influx}} \cdot C_p - k_{\text{efflux}} \cdot C_e$, in which

[1] Division of Bioengineering and Physical Science, Office of Research Services, National Institutes of Health, Bethesda, Maryland 20892.
[2] Pediatric Oncology Branch, Division of Clinical Sciences, National Cancer Institute, National Institutes of Health, Bethesda, Maryland 20892.
[3] To whom correspondence should be addressed at DBEPS/NIH, Building 13/3N17, MSC 5766, Bethesda, Maryland 20892-5766. (e-mail: bungayp@mail.nih.gov)

k_{influx} and k_{efflux} are unidirectional exchange rate constants and C_e is the local free concentration in the ECF. The exchange rate constants are calculated from the following relationships and values given to the corresponding microvascular permeability-area products per gram of tissue, ps_{influx} and ps_{efflux},

$$k_{influx} = Q_p \cdot (1 - e^{-ps_{influx}/Q_p}), \quad (2)$$

and,

$$k_{efflux} = Q_p \cdot (1 - e^{-ps_{efflux}/Q_p}), \quad (3)$$

where $Q_p = Q_b \cdot \Phi_b$, the effective plasma flow rate per gram of tissue, is the product of the blood flow rate per gram of tissue, Q_b, and the blood-to-plasma distribution coefficient, Φ_b. We will use units of ml/(hr · g tiss) for the rate constants and other parameters in Eqs. (2) and (3). The units employed for the rate constants in MICRODIAL are ml/(hr · ml ECF). The ECF volume fraction, ϕ_e, in units of ml ECF/g tiss serves as a conversion factor between ECF volume and tissue mass.

For the transient model, MICRODIAL generates values of the free analyte concentration in the distant ECF, $C_e^{\infty}[t]$, and the instantaneous dialysate extraction fraction, $E_d[t]$, as a function of time. The extraction fraction is a measure of the degree of equilibration between the dialysate and the ECF. This calibration factor is defined as the ratio,

$$E_d[t] = \frac{C_{in} - C_{out}[t]}{C_{in} - C_e^{\infty}[t]}, \quad (4)$$

where C_{in} and C_{out} are the concentrations of the analyte in the incoming perfusate and exiting dialysate, respectively. The extraction fraction is a generalized form of the quantity often termed relative recovery. For microdialysis sampling, no analyte is added to the inflowing perfusate, so $C_{in} = 0$ and the extraction fraction from Eq. (4) reduces to,

$$E_d[t] = C_{out}[t]/C_e^{\infty}[t]. \quad (5)$$

A time-dependent variation in the extraction fraction, designated above as a mass transfer transient, is created when the microdialysis system is perturbed by changing C_{in} or the dialysate flow rate, Q_d. Perturbations in C_{in} or Q_d will result in time variation in C_{out}, but not C_e^{∞}. The time variation in C_e^{∞} is a manifestation of the pharmacokinetic transient produced by unsteady supply, clearance and exchange processes. The variation in C_e^{∞} induces both mass transfer and pharmacokinetic components in the resulting transient changes in C_{out} and E_d.

RESULTS

We have employed the transient, cylindrical geometry model of MICRODIAL to examine the characteristics of microdialysis transients. First we present the results for pure mass transfer transients *in vivo,* and then we consider the combined mass transfer and pharmacokinetic transients occurring in *in vivo* experiments involving changes in the distant ECF concentration, C_e^{∞}. The hypothetical set of parameter values in Table I was used for the simulations. The values are representative of a non-binding solute of molecular weight of the order of 300 Daltons exchanging between the dialysate and brain ECF. The microdialysis probe is perfused at 1 μl/min. The choice of a 1-cm long membrane length derives from experiments in the cortex of rhesus monkeys. Most parameters, such as perfusion rate and membrane length, were assigned fixed values, since they have little influence on the rapidity of the mass transfer transient. Parameters assigned a range of values were the key rate constants: ECF-to-plasma efflux (k_{efflux}), plasma-to-ECF influx (k_{influx}), first order degradation in the ECF (k_e^r), and plasma decay (λ).

Table I. Microdialysis Parameters

Symbol	Values	Units	Description
r_α	0.012	cm	Inner cannula radius
r_i	0.020	cm	Membrane inner radius
r_o	0.025	cm	Membrane outer radius
L_m	1.0	cm	Membrane length
$D_m\phi_m$	0.6×10^{-4}	cm^2/min	Effective analyte diffusion coefficient in probe membrane at 37°C
D_d	4.5×10^{-4}	cm^2/min	Analyte diffusion coefficient in free solution at 37°C
Q_d	1	μl/min	Perfusate volumetric flow rate
ϕ_e	0.2	ml ECF/g tiss	Extracellular volume fraction
D_e	1.8×10^{-4}	cm^2/min	Analyte diffusion coefficient in ECF at 37°C
ps_{influx}	0.1–10	ml/(hr · g tiss)	Permeability-area product for influx to tissue
ps_{efflux}	0.1–10	ml/(hr · g tiss)	Permeability-area product for efflux from tissue
Q_p	60	ml/(hr · g tiss)	Effective plasma volumetric flow rate
C_{pO}	1		Initial analyte concentration in plasma ($t = 0$)
C_{eO}	0		Initial analyte concentration in ECF ($t = 0$)
C_{in}	0, 1		Analyte concentration in inflowing perfusate
k_i^r	0		Rate constant for intracellular degradation
k_e^r	0, 1	ml/(hr · g tiss)	Rate constant for extracellular degradation
R_i''	1		Intracellular binding coefficient
R_e''	1		Extracellular binding coefficient
K_π	1		Intracellular/extracellular analyte partition coefficient
λ	0, 1	hr^{-1}	Rate constant for analyte plasma disappearance

Note: All tissue densities assigned the value of 1 g/ml. The extracellular volume fraction serves as a conversion factor for basing rate constants on either tissue mass or ECF volume.

Mass Transfer Transients

Figure 1 illustrates that the magnitude and rapidity of transients in the extraction fraction are strongly influenced by the coupling between analyte diffusion and clearance processes in the ECF in the vicinity of the probe. The examples shown represent the extraction fraction transient that occurs when probe perfusion is initiated at time = 0. We assume the analyte ECF concentration is spatially uniform before this change. As a consequence of the assumption of linearity in concentration, the results apply to either analyte sampling (C_e^∞ = constant, C_{in} = 0) or analyte delivery to the tissue via the probe perfusate (C_{in} = constant, C_e^∞ = 0). The clearance rate constant, k_{clr}, represents the sum of the rate constants for efflux and degradation. The arbitrary values of k_{clr}, 0.1–10 ml/(hr · g tiss), cover a physiologically meaningful range from moderately slow to moderately fast clearance by microvascular efflux from the brain ECF. For comparison, sucrose is slowly cleared from the brain with an efflux rate constant estimated to be 0.02 ml/(hr · g tiss) (4). For fast blood-flow limited efflux from the brain, k_{clr} would be of the order of 60 ml/(hr · g tiss), based on a representative value for blood flow to the brain of 1 ml(min · g tiss)$^{-1}$ (6). Orders of magnitude faster ECF clearance rates are estimated for some processes, such as enzymatic degradation or active transport of neurotransmitters.

The reason for the time course of E_d, starting with a high initial level at time = 0 and falling to the steady-state value is suggested in Fig. 2 for the sampling case. The figure displays radial concentration profiles within the dialysate, membrane and ECF for various times for the case of k_{clr} = 1 ml/(hr · g tiss). The concentration difference across the probe membrane is a maximum at time = 0 because the analyte concentration is uniform throughout the ECF. The rapid diffusive flux of analyte across the membrane at that moment gives rise to the initial elevated E_d value. As analyte is drained from the tissue, the concentration difference and the flux across the membrane decrease progressively with time. Concomitantly, E_d decreases monotonically towards a steady-state value corresponding to a steady-state concentration profile within the tissue and probe.

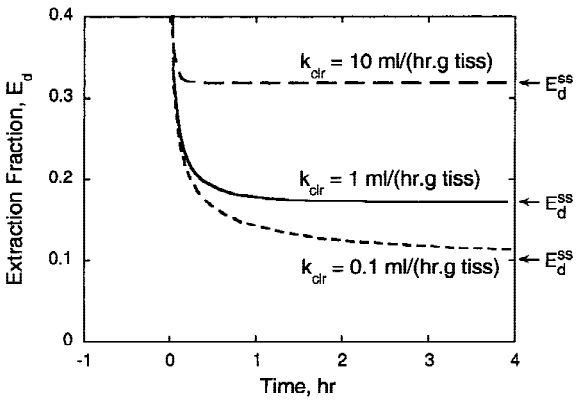

Fig. 1. Mass transfer transient in the calibration factor (E_d) for initiating microdialysis sampling of analyte from tissue (C_e^∞ = constant, C_{in} = 0) or for delivery of analyte to tissue from the probe perfusate (C_{in} = constant, C_e^∞ = 0). The arrows to the right indicate the values of the respective steady-state calibration, E_d^{ss}. The curves represent simulations that differ in the value for the overall rate constant for analyte clearance from the tissue interstitium, k_{clr}. Other parameter values provided in Table I.

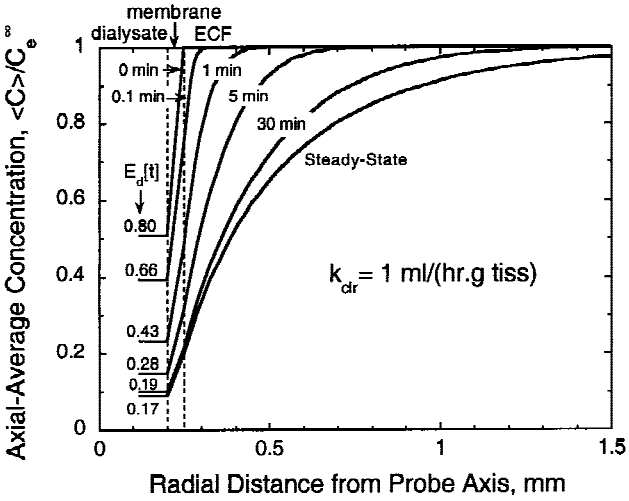

Fig. 2. Radial profiles of analyte concentration in the dialysate, membrane and extracellular fluid (ECF) corresponding to the mass transfer transient of Fig. 1 for the case of analyte sampling and k_{clr} = 1 ml/(hr · g tiss). The concentrations have been averaged over the length of the membrane as indicated by the brackets, < >. The concentration variation is mostly within the membrane at early times and primarily within the tissue at later times.

There are two predominant trends in the E_d transients in Fig. 1. All else being equal, lowering the value of k_{clr} decreases E_d and slows the approach to steady state. The first trend is significant, but the 100-fold range in k_{clr} only produces about a 3-fold change in the steady-state E_d. The second trend is more pronounced. The transient E_d is within 10% of its steady-state level after only 4 min for a k_{clr} of 10 ml/(hr · g tiss), but at k_{clr} = 0.1 ml/(hr · g tiss), E_d takes more than 4 hr to approach within 10% of its steady-state value.

Combined Mass Transfer and Pharmacokinetic Transients

We have simulated two kinds of idealized *in vivo* microdialysis sampling experiments. Both cases involve systemic administration of the agent to be sampled. The compartmental analyte concentration-time profiles are displayed in Fig. 3. The first case (*iv infusion,* Fig. 3A) represents a loading dose followed by a programmed continuous infusion of the agent to achieve a step change in C_p. In the second case (*iv bolus,* Fig. 3B), an instantaneous unit change in C_p is imposed followed by a monoexponential decline over time with a decay constant value of λ = 1 hr^{-1}, which is of the order of magnitude of that observed for zidovudine (AZT) (7,8).

For simplicity in displaying the results, we show only situations in which efflux to blood is the sole mechanism for analyte clearance from the ECF (k_{clr} = k_{efflux}), and blood-tissue exchange is symmetric (k_{influx} = k_{efflux}). In both cases, the rate constants are arbitrarily set to the values, k_{clr} = k_{influx} = k_{efflux} = 1 ml/(hr · g tiss). However, the conclusions about the nature of the microdialysis transients apply to the more general situations in which analyte is simultaneously cleared from the ECF by degradation and oriented transport mechanisms that result in asymmetric exchange. For comparison, the rate constant for zidovudine clearance from rat striatum was estimated to be k_{clr} = k_{efflux} = 0.8 ml/(hr · g tiss) (9).

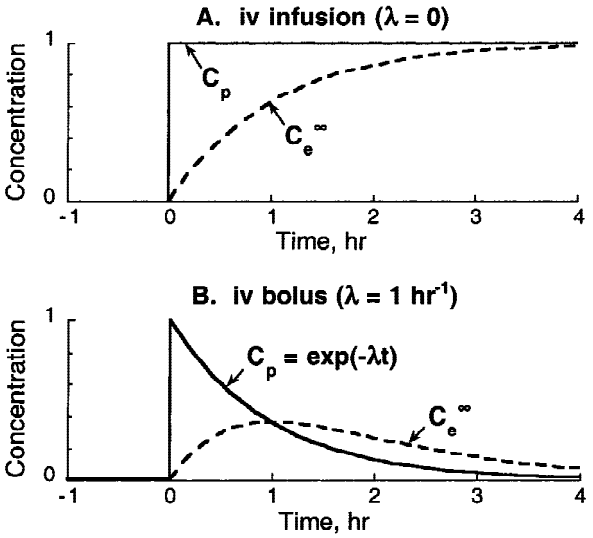

Fig. 3. Simulated pharmacokinetic experiments used to predict differences in the transient microdialysis calibration factor when the distant free extracellular analyte concentration (C_e^∞) varies over time. A. *iv infusion:* Intravenous loading dose plus programmed infusion of analyte to cause a step change in the free plasma concentration (C_p). Symmetric plasma-to-tissue exchange has been specified ($k_{\text{influx}} = k_{\text{efflux}} = 1$ ml/(hr · g tiss)$^{-1}$), so that at steady state, $C_e^\infty = C_p$. B. *iv bolus:* Intravenous bolus administration of analyte followed by a monoexponential decline in free plasma concentration for a decay rate constant of $\lambda = 1$ hr^{-1}. Except for λ, the parameter values are the same as for the *iv infusion* case (see Table I).

iv Infusion

The step change in C_p produces an exponential transient in C_e^∞ (Fig. 3A), which approaches C_p at long times because of the imposed symmetry in exchange, $k_{\text{influx}} = k_{\text{efflux}}$. Since C_e^∞ achieves a non-zero steady state, the transient E_d profile shown in Fig. 4 approaches the same steady-state level as for the mass transfer transient (middle curve of Fig. 1). However, the combined mass transfer and pharmacokinetic transient in E_d in the infusion case is slower than that of the corresponding pure mass transfer transient in Fig. 1.

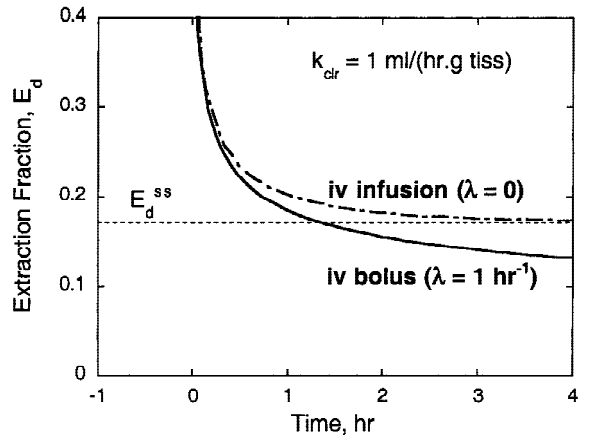

Fig. 4. Combined mass transfer and pharmacokinetic transients in the microdialysis calibration factor, E_d, for the simulated experiments from Fig. 3. Also shown for the *iv infusion* case is the steady-state value (dashed line), which is the same as the E_d^{ss} value indicated in Fig. 1 for $k_{\text{clr}} = 1$ ml/(hr · g tiss). Although the microdialysis parameter values are the same, the *iv infusion* and *iv bolus* transients in E_d differ from one another, and from the corresponding pure mass transfer transient of Fig. 1.

iv Bolus

At long times the compartmental concentrations, C_e^∞ and C_p, return to zero (Fig. 3B). However, C_e^∞ lags C_p producing the unexpected result shown in Fig. 4. For most of the experiment, E_d is lower than the mass transfer steady-state E_d level. As in the *iv infusion* case, the transient in E_d is slower than that of the corresponding pure mass transfer transient in Fig. 1.

DISCUSSION

In the pure mass transfer transient, E_d for $k_{\text{clr}} = 10$ ml/(hr · g tiss) approaches steady state on the time scale of a typical 10-min microdialysis sampling interval (Fig. 1). However, at the low clearance rate of $k_{\text{clr}} = 0.1$ ml/(hr · g tiss), several hours are required to achieve steady state. Furthermore, the steady-state E_d is likely to be difficult to ascertain experimentally because the time course does not exhibit a simple exponential decay.

The E_d curves for the *iv infusion* and *iv bolus* cases in Fig. 4 were produced for identical microdialysis parameter values (Table I). The only difference between them is in the time course of the compartmental concentrations, C_p and C_e^∞. This illustrates the point that the transient in E_d depends on the nature of the pharmacokinetic experiment, as well as the microdialysis parameters. This suggests that methods for calibration in transient experiments for probes in solid tissues may be severely limited.

As an illustration of the problem this poses for transient calibration, consider retrodialysis approaches in which a surrogate marker solute is added to the probe perfusate. If the marker solute is neither initially present in the tissue ($C_e^\infty = 0$), nor systemically administered ($C_p = 0$), the marker solute will exhibit a pure mass transfer transient E_d of the kind shown in Fig. 1 that can be followed experimentally by monitoring $C_{\text{out}}[t]$,

$$(E_d[t])_{\text{retro}} = 1 - (C_{\text{out}}[t]/C_{\text{in}}). \quad (6)$$

Requiring that the microdialysis parameters of the marker solute agree with those of the analyte will achieve equality in the steady-state value of E_d for the two solutes. However, the transient E_d time course of the two solutes will agree only if, in addition, both solutes have the same plasma kinetics and are administered systemically in identical fashion, i.e. concurrently at the same location. If they were so administered, then C_e^∞ for the marker solute will be non-zero during the course of the experiment and $E_d[t]$ cannot be obtained from Eq. (6) with measurements of just C_{in} and $C_{\text{out}}[t]$.

One possibility for maintaining a known calibration during transient experiments is the limiting situation of operating at E_d close to unity at all times by slow perfusion. This option sacrifices information about tissue processes obtainable from E_d. The one general approach proposed for determining the variation in E_d during an experiment is the transient no-net-flux technique of Olson and Justice (10). One concern that restricts the practicability of this technique is the number of

animals required for the necessary between-group comparisons.

In some pharmacokinetic experiments, it is not necessary to determine the time course of C_p and C_e^∞. Rather, it suffices to obtain the time integral of these concentrations, i.e.,

$$AUC_{0-\infty} = \int_0^\infty C[t] \cdot dt. \tag{7}$$

For systems exhibiting linear dependence on analyte concentration, it seems that the $AUC_{0-\infty}$ for either C_e^∞ or C_p can be obtained by microdialysis from the time integrals of the respective $C_{out}[t]$ integrals. The dialysate and *in vivo* concentration integrals appear to be proportionally related by the steady-state E_d values according to,

$$AUC_{0-\infty} = \left(\int_0^\infty C_{out}[t] \cdot dt \right) / E_d^{SS}. \tag{8}$$

This relationship has been substantiated empirically by MICRODIAL simulations for the parameter values of Table 1 and a wide range of values of k_{influx}, k_{efflux}, and λ.

The microdialysis requirements for Eq. (8) can represent a significant experimental simplification, since the right-hand-side contains only two quantities, $\int_0^\infty C_{out}[t] \cdot dt$ and E_d^{ss}. In principal, each of these quantities can be obtained from a single dialysate sample, provided E_d^{ss} is a constant over the course of the pharmacokinetic experiment. The probe calibration factor, E_d^{ss}, can be determined before or after the pharmacokinetic experiment by a steady-state technique. The dialysate integral can be approximated from the concentration in a pooled dialysate collected over the duration, T, of the pharmacokinetic experiment. For sufficiently large T,

$$\int_0^\infty C_{out}[t] \cdot dt \approx \int_0^T C_{out}[t] \cdot dt = T \cdot C_{out}^{pooled}. \tag{9}$$

Alternatively, the dialysate integral in Eqs. (8) and (9) can be obtained from multiple, successive samples taken during the experiment, rather than from a single continuous sample.

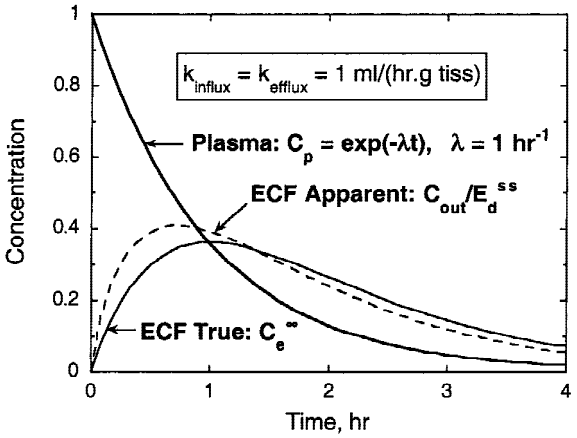

Fig. 5. Analyte concentration-time profiles for *iv bolus* administration of analyte followed by a monoexponential decline in free plasma concentration ($\lambda = 1\ hr^{-1}$). The solid curves are the free plasma (C_p) and distant free extracellular concentration (C_e^∞) profiles from Fig. 3B. The dashed curve is the apparent free extracellular concentration profile estimated from the effluent dialysate concentration (C_{out}) and the steady-state value of the calibration factor (E_d^{ss}). The values of the concentration-time integrals, $AUC_{0-\infty}$, for all three curves are the same.

Although E_d^{ss} properly converts the dialysate integral to $AUC_{0-\infty}$, this steady-state calibration factor does not correctly convert the concentration in individual dialysate samples. This point is illustrated in Fig. 5 by the *iv bolus* case for $k_{influx} = k_{efflux} = 1$ ml/(hr · g tiss). The C_e^∞ and C_p time courses from Fig. 3 for this case are replotted in Fig. 5 as the solid curves. The dashed curve represents the apparent C_e^∞ estimated as $C_{out}[t]/E_d^{ss}$. At early times the apparent C_e^∞ estimates exceed the true values, because $E_d^{ss} < E_d[t]$ as shown by the *iv bolus* extraction fraction curve in Fig. 4. At later times the extraction fraction inequality is reversed and $C_{out}[t]/E_d^{ss}$ underestimates the true C_e^∞. The apparent and true ECF concentrations agree only at the time for which the $C_{out}[t]/E_d^{ss}$ and C_e^∞ curves cross. However, the area under both curves, if extended to infinite time, would be the same and equal to $AUC_{0-\infty}$. The AUC values from $t = 0$ to $t = T$ will differ to an extent that depends upon the proportion of $AUC_{0-\infty}$ that is truncated for each variable. In the example of Fig. 5, the 0–4 hr integrals are 93.5% and 91.0% of $AUC_{0-\infty}$ for the apparent ECF and true ECF concentrations, respectively.

The discrepancy between C_{out}/E_d^{ss} and C_e^∞ is a function of the relative magnitudes of the rate constants for plasma decay, λ, and microvascular exchange, k_{influx} and k_{efflux}. This is illustrated by the results of a sensitivity analysis displayed in

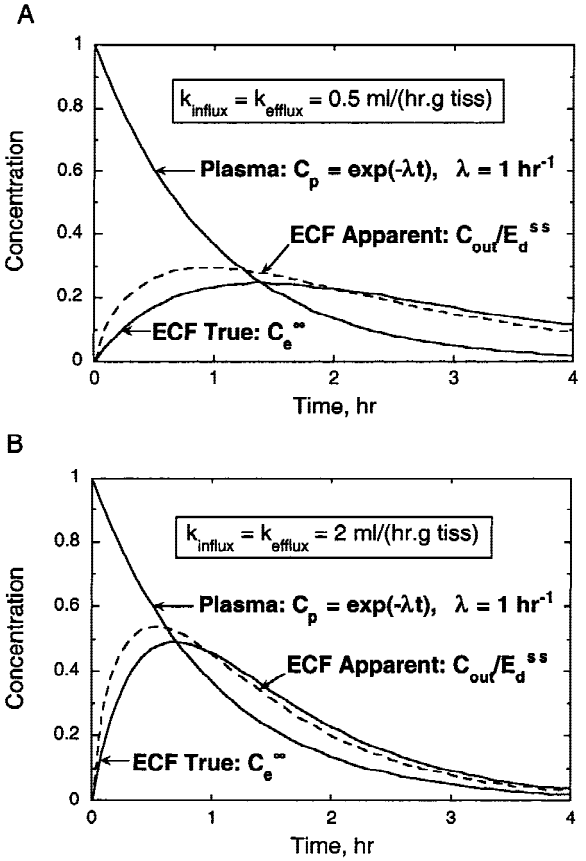

Fig. 6. Sensitivity analysis for the influence of microvascular exchange rate constants on the apparent free extracellular concentration (C_{out}/E_d^{ss}) of analyte following *iv bolus* administration. The parameter values employed in the simulations were the same as for Fig. 5 except (A) $k_{influx} = k_{efflux} = 0.5$ ml/(hr · g tiss) and (B) $k_{influx} = k_{efflux} = 2$ ml/(hr · g tiss). The values of the concentration-time integrals, $AUC_{0-\infty}$, for all of the curves in A, B and Fig. 5 are equal.

Fig. 6 in which the *iv bolus* simulation of Fig. 5 was repeated for two different values of $k_{influx} = k_{efflux}$ while keeping the values of λ and the other parameters fixed. The exchange rate constants have a strong influence on the peak concentrations and the time at which the peak occurs. Again, the $AUC_{0-\infty}$ is the same for all of the curves in Figs. 5 and 6 as predicted by Eq. (8). However, the discrepancy between the C_{out}/E_d^{ss} and C_e^{∞} curves is only weakly affected by varying these rate constants. This weak dependence arises from two offsetting effects: increasing $k_{clr} = k_{efflux}$ results in a more rapid mass transfer transient (as in Fig. 1), while increasing k_{influx} and k_{efflux} produces a more rapid pharmacokinetic transient (Figs. 5 and 6). Thus, the increase in rapidity of the microdialysis response (C_{out}) is not enough to compensate for the faster transient in C_e^{∞}.

The mathematical models used for this analysis assume that analyte moves through the tissue and the probe membrane only by diffusion. For probes placed in blood or other fluid media, the models are appropriate only if diffusion predominates over convective transport of analyte in the vicinity of the probe (i.e., if the fluid surrounding the probe is essentially quiescent). Since this may not be the case, the applicability of this transient analysis to probes in fluid media is uncertain. Convection through the probe membrane is usually assumed to be negligible, so the contribution of the membrane to the mass transfer transient in E_d will be present for probes in any medium. However, the formulation of the transient model in the current version of MICRODIAL treats the membrane as a diffusional resistance that has no mass (2). This simplification should not invalidate Eq. (8), but including analyte mass in the membrane would tend to slow both mass transfer and pharmacokinetic transients. The effect on the simulations in the present analysis for probes in solid tissues would probably be small. By contrast, for a probe immersed in a well-stirred fluid, the membrane would be the dominant contributor to E_d transients.

In summary, we have shown by illustrative simulations that practicable general techniques for measuring extracellular concentrations in solid tissues by microdialysis are limited in transient experiments. On the other hand, we propose that $AUC_{0-\infty}$ concentration-time integrals can be obtained for linear systems by simplified microdialysis procedures based on Eq. (8). Because of a current limitation in the simulation program, MICRODIAL, validation of this proposal has been restricted to date to the *iv bolus* case with a monoexponential decline in plasma concentration and single compartment behavior for the ECF. However, Eq. (8) appears to be valid in the presence of analyte degradation and asymmetric tissue-to-plasma exchange provided the rates of these processes also depend linearly on analyte concentration (results not presented). Thus, the proposed method for $AUC_{0-\infty}$ determination by microdialysis may have more general applicability.

REFERENCES

1. P. F. Morrison, P. M. Bungay, J. K. Hsiao, B. A. Ball, I. N. Mefford, and R. L. Dedrick. Quantitative microdialysis: Analysis of transients and application to pharmacokinetics in brain. *J. Neurochem.* **57**:103–119 (1991).
2. P. F. Morrison, P. M. Bungay, J. K. Hsiao, I. N. Mefford, K. H. Dykstra, and R. L. Dedrick. Quantitative microdialysis. In T. E. Robinson and J. B. Justice, Jr. (eds.), *Microdialysis in the Neurosciences,* Elsevier, New York, 1991 pp. 47–80.
3. J. A. Stenken. Methods and issues in microdialysis calibration. *Anal. Chim. Acta.* **379**:337–358 (1999).
4. P. M. Bungay, P. F. Morrison, and R. L. Dedrick. Steady-state theory for quantitative microdialysis of solutes and water *in vivo* and *in vitro. Life Sci.* **46**:105–119 (1990).
5. P. F. Morrison, P. M. Bungay, and C. R. Swyt. MICRODIAL 1.0, Bethesda, Maryland, 1991.
6. O. Sakurada, C. Kennedy, J. Jehle, J. D. Brown, G. L. Carbin, and L. Sokoloff. Measurement of local cerebral blood flow with iodo [14C] antipyrine. *Am. J. Physiol.* **234**:H59–H66 (1978).
7. F. M. Balis, P. A. Pizzo, R. F. Murphy, J. Eddy, P. F. Jarosinski, J. Falloon, S. Broder, and D. G. Poplack. The pharmacokinetics of zidovudine administered by continuous infusion in children. *Ann. Intern. Med.* **110**:279–285 (1989).
8. B. A. Patel, F. D. Boudinot, R. F. Schinazi, J. M. Gallo, and C. K. Chu. Comparative pharmacokinetics and interspecies scaling of 3′-azido-3′-deoxythymidine (AZT) in several mammalian species. *J. Pharmacobiodyn.* **13**:206–211 (1990).
9. K. H. Dykstra, A. Arya, D. M. Arriola, P. M. Bungay, P. F. Morrison, and R. L. Dedrick. Microdialysis study of zidovudine (AZT) transport in rat brain. *J. Pharmacol. Exp. Ther.* **267**:1227–1236 (1993).
10. R. J. Olson and J. B. Justice, Jr. Quantitative microdialysis under transient conditions. *Anal. Chem.* **65**:1017–1022 (1993).